Radiation Measurements 177 (2024) 107270

Contents lists available at ScienceDirect

Radiation Measurements

journal homepage: www.elsevier.com/locate/radmeas

Optically stimulated luminescence detectors for LET determination and dosimetry in ion beam therapy

Jeppe Brage Christensen [a,*], Lily Bossin [a], Iván Domingo Muñoz [b,c,d], Christina Stengl [e,c,d], José Vedelago [f,c,d], Eduardo Gardenali Yukihara [a]

[a] Department of Radiation Safety and Security, Paul Scherrer Institut (PSI), Villigen PSI, Switzerland
[b] Department of Physics and Astronomy, University of Heidelberg, Heidelberg, Germany
[c] Division of Medical Physics in Radiation Oncology, German Cancer Research Center (DKFZ), Heidelberg, Germany
[d] Heidelberg Institute for Radiation Oncology (HIRO) and National Center for Radiation Research in Oncology (NCRO), Heidelberg, Germany
[e] Faculty of Medicine, University of Heidelberg, Heidelberg, Germany
[f] Department of Radiation Oncology, Heidelberg University Hospital (UKHD), Heidelberg, Germany

ARTICLE INFO

Keywords:
Optically stimulated luminescence
Linear energy transfer
Ion beam therapy
Dosimetry

ABSTRACT

Optically stimulated luminescence detectors (OSLDs) have been utilized for various dosimetry applications for many years. The use of Al_2O_3:C OSLDs for proton dosimetry began over a decade ago, taking advantage of the correlation between the ionization density of the radiation field and the ratio of intensities of the material's two emission bands. The correlation allows for determining both linear energy transfer (LET) and dose in proton beams, with corrections for ionization quenching derived from the LET. However, the previous methodology for proton dosimetry and simultaneous LET determination with Al_2O_3:C OSLDs was cumbersome and occasionally associated with large uncertainties, while carbon beam dosimetry posed further challenges due to an elevated LET.

This paper reviews the recent advancements in ion beam dosimetry and LET determination using OSLDs. Employing Al_2O_3:C,Mg OSLDs alongside improved, automatized read-out techniques, and the use of other radiation quality metrics than averaged LET, has removed most of the previous obstacles for ion beam dosimetry with OSLDs.

The feasibility of simultaneous LET determination and dosimetry in ion beams is demonstrated through two case studies involving realistic proton and carbon ion therapy scenarios.

1. Introduction

Optically stimulated luminescence (OSL) has been used for dosimetry for decades (Yukihara et al., 2022b). The utilization of Al_2O_3:C OSL detectors (OSLDs) has been widespread, notably in medical dosimetry for photon fields (Edmund et al., 2006), radiation fields relevant to space dosimetry (Yasuda and Kobayashi, 2001), and later extended to include dosimetry for ion beam therapy (Sawakuchi et al., 2008).

Al_2O_3:C OSLDs exhibit two emissions upon stimulation, one in the blue optical emission band and one in the ultraviolet (UV) band, attributed to F- and F^+-center emissions, respectively (Yukihara et al., 2006). Historically, the emphasis has been on using the blue emission band centered at 420 nm for dosimetry due to its favorable luminescence properties and minimal fading rate.

However, the relative luminescence efficiency of this band decreases with increasing linear energy transfer (LET) relevant to ion beams, necessitating ionization quenching corrections for the often unknown average LET ($\overline{\text{LET}}$) of the particle spectrum at the detector position (Sawakuchi et al., 2010). In contrast, the relative emission intensity of the UV band may increase with both time and $\overline{\text{LET}}$ (Granville et al., 2014; Granville, 2015), requiring larger correction factors for dosimetry compared with the blue emission band. For comparison, OSLDs based on MgB_4O_7:Ce,Li have been demonstrated to be almost quenching-free in clinically relevant proton beams (Yukihara et al., 2022a).

Al_2O_3:C OSLDs' potential to identify high- or low-LET components in radiation fields with heavy charged particles was proposed by Yukihara and McKeever (2006). It was later demonstrated that the OSLDs can be used to determine $\overline{\text{LET}}$ in clinically relevant proton beams by Sawakuchi et al. (2010), linking the shape of the OSL intensity as a function of stimulation time to both fluence-averaged LET ($\overline{\text{LET}}_\text{F}$) and dose-averaged LET ($\overline{\text{LET}}_\text{D}$). This determination was refined by Granville

* Corresponding author.
E-mail address: jeppe.christensen@psi.ch (J.B. Christensen).

https://doi.org/10.1016/j.radmeas.2024.107270
Received 22 February 2024; Received in revised form 28 June 2024; Accepted 12 August 2024
Available online 13 August 2024
1350-4487/© 2024 The Author(s). Published by Elsevier Ltd. This is an open access article under the CC BY license (http://creativecommons.org/licenses/by/4.0/).

et al. (2014), who demonstrated that the ratio of UV to blue emission band intensities correlates better with $\overline{\text{LET}}$ than the OSL curve shape does. Furthermore, separating the UV and blue emission bands was previously demonstrated by Yukihara and McKeever (2006) to be achievable without spectroscopic tools by utilizing their distinct lifetimes, which can be differentiated through the so-called pulsed-OSL technique. Based on these findings, Yukihara et al. (2015) proceeded to characterize the response of both emission bands in light ion beams relevant to radiotherapy as a function of $\overline{\text{LET}}_{\text{D}}$.

Using the ratio of UV to blue emission bands for $\overline{\text{LET}}$ determinations enabled corrections for ionization quenching relevant to ion beams for improved dosimetry. Indeed, with relative detector efficiency characterization, the determined $\overline{\text{LET}}$ can provide a correction factor for ionized quenched detector response. Therefore, this approach allows simultaneous determination of both $\overline{\text{LET}}$ and dose with a single detector, with the dose subject to an ionization quenching correction derived from the $\overline{\text{LET}}$. The feasibility of this simultaneous determination was highlighted for proton dosimetry by Granville et al. (2016).

However, employing OSLDs for dosimetry and $\overline{\text{LET}}$ determination in light ion beams has presented several challenges:

(i) The relationship between the UV/blue ratio and $\overline{\text{LET}}$, referred to as the LET calibration, is highly non-linear. Even small uncertainties in UV/blue determination can propagate to relatively larger uncertainties in $\overline{\text{LET}}$ determination, adversely affecting the accuracy of the dosimetry. This previous spread of the UV/blue ratios from OSLDs irradiated with the same radiation quality necessitated a more precise determination of the UV/blue emission ratio. An improvement was explored using the S/S_R technique outlined below, wherein the signal from each OSLD underwent correction through reference irradiation and readout (Yukihara et al., 2005).

(ii) Yukihara et al. (2015) showed that the response of Al_2O_3:C OSLDs irradiated with ions heavier than helium only correlates vaguely with the $\overline{\text{LET}}$. This points towards the need for a better OSL material for $\overline{\text{LET}}$ determination in carbon ion therapy. To address this challenge, the OSLD material Al_2O_3:C,Mg (Akselrod and Akselrod, 2006) was investigated for improved $\overline{\text{LET}}$ determinations (Christensen et al., 2023).

(iii) Previously, dose corrections for ionization quenching have mainly been determined through the commonly used radiation quality metric $\overline{\text{LET}}_{\text{F}}$ or mainly $\overline{\text{LET}}_{\text{D}}$. As this approach shows limitations, the radiation quality metric Q_{eff}, which is related to the track structure of ions, was investigated in an attempt to improve the dosimetry (Christensen et al., 2023).

The objective of this review paper is to outline the recent improvements and to compile the current knowledge of $\overline{\text{LET}}$ determination and dosimetry using OSLDs for proton and light ion beam therapy. The potential of using OSLDs for quality assurance for proton and carbon ion beam therapy was demonstrated by simultaneous $\overline{\text{LET}}$ and dose determination in anthropomorphic phantoms.

2. Improving the accuracy of ion beam dosimetry with OSLDs

Dosimetry with Al_2O_3:C OSLDs is well-documented in the literature and enables precision better than 1% using the so-called S/S_R approach (Yukihara et al., 2005; Motta et al., 2023). The S/S_R technique takes advantage of the presence of a radiation source in some luminescence readers. Following the OSL readout of the detector's signal, S, the detector undergoes irradiation in the reader with a known dose, followed by another subsequent readout of the signal, S_R. Consequently, the ratio S/S_R eliminates material sensitivity differences or variations in detectors' size. Recently, the method was applied to both demonstrate that Al_2O_3:C is the most precise luminescence detector commercially available (Motta et al., 2024) as well as being dose-rate independent at ultra-high dose rate electron beams (Motta et al., 2024) and proton beams (Christensen et al., 2021).

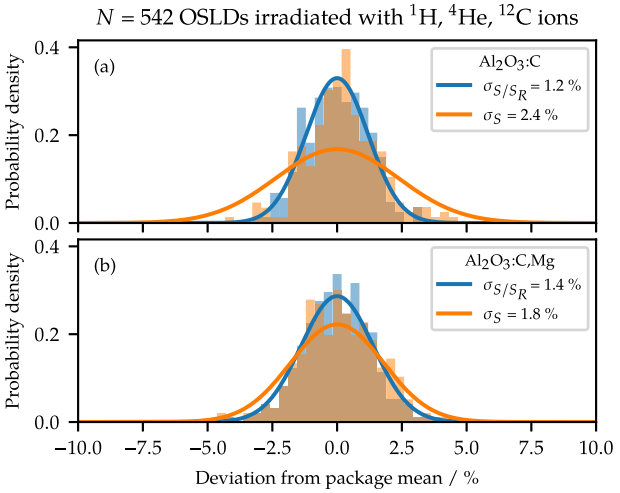

Fig. 1. The spread of the UV/blue emission ratio, where the deviation is calculated relative to the mean value of a given package, which contained 3 to 8 OSLDs. The deviation of the package mean is calculated for both the UV/blue ratio (S) and for the case the UV/blue ratios each are scaled by the signal from the reference irradiation (S/S_R). (a) shows the results for Al_2O_3:C and (b) for the Al_2O_3:C,Mg OSLDs.

Although the ratio of UV and blue emission intensities inherently mitigates many differences between OSLDs within a batch, we showed that the precision of UV/blue determination can be further enhanced using a similar S/S_R protocol (Christensen et al., 2022).

Fig. 1 illustrates the spread of 542 OSLDs grouped in different packages. The dataset shows the deviation from each package mean and encompasses OSLDs irradiated with different ions, namely ^{1}H, ^{4}He, and ^{12}C ions at doses between 0.1 Gy to 1.5 Gy. For both the Al_2O_3:C OSLDs in Fig. 1a and Al_2O_3:C,Mg OSLDs in Fig. 1b, using the UV/blue ratio corrected by the reference irradiation, S/S_R, yields the highest precision. Although the improvement for Al_2O_3:C,Mg from 1.8% to 1.4% is relatively small, the S/S_R technique represents a step towards more precise determination of radiation quality correction factors to refine dosimetry.

Due to the non-uniformity of certain fields used to acquire the data, the spread of data in Fig. 1 exceeds the spread reported in Yukihara et al. (2005) or Christensen et al. (2022).

3. Characteristics of Al_2O_3:C and Al_2O_3:C,Mg OSLDs

Both Al_2O_3:C and Al_2O_3:C,Mg OSLDs were prepared from a <100 μm film developed by Landauer Inc. (Ahmed et al., 2014). The OSL films consist of a (50 ± 3) μm layer of Al_2O_3 grains mixed with a binder and applied to a polyester substrate. The water-equivalent thickness (WET) of the OSLD foils has not yet been precisely determined but typically remains unaccounted for due to their thinness and the predominant polyester composition, which results in a WET at a sub-millimeter scale. The OSLDs were cut to diameters ranging between 1 mm to 7 mm across all studies.

3.1. Dose response

The determination of $\overline{\text{LET}}$ with OSLDs is influenced by various parameters, with the two most significant being the effect of overlapping ion tracks, i.e. the dose, and signal fading or build-up over time. Here, these factors are emphasized for Al_2O_3:C,Mg and compared to the properties of Al_2O_3:C. The dose responses of the UV/blue emission ratio for both Al_2O_3:C and Al_2O_3:C,Mg OSLDs irradiated with 230 MeV protons are shown in Fig. 2a.

The overlapping ion tracks perturb the ionization density in neighboring tracks. This increased ionization density affects the UV/blue

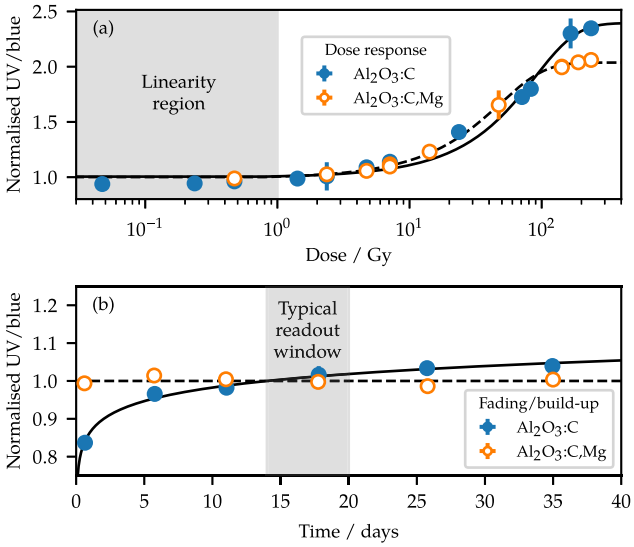

Fig. 2. (a) Dose response to 230 MeV protons of Al_2O_3:C and Al_2O_3:C,Mg OSLDs for the UV/blue emission ratio which is used for LET determination. Logistic functions are fitted to the data merely to guide the eye. (b) The response of the UV/blue emission ratio as a function of time after readout. The readouts of the OSLDs of both materials are typically first started 14 days after irradiation to mitigate the effects of the signal variation with time. The legend in (a) is representative for both (a) and (b).
Source: Fading and build-up data adapted from Christensen et al. (2022).

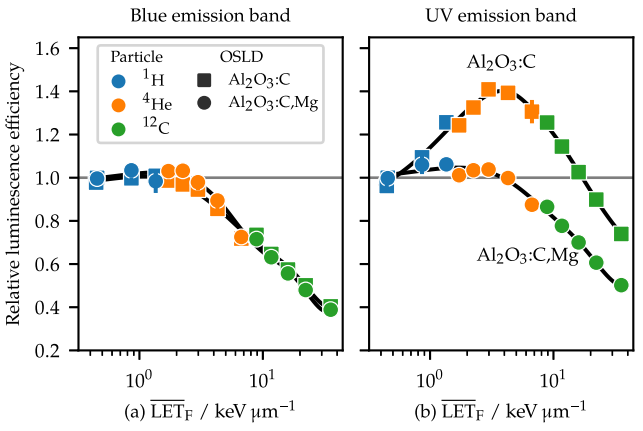

Fig. 3. The relative luminescence efficiency of (a) the blue emission band and (b) the UV emission band during stimulation after irradiation with light ions at different ionization densities calculated as $\overline{LET}_F$ in water. Whereas the blue emission band exhibits a similar structure for Al_2O_3:C and Al_2O_3:C,Mg OSLDs, the relative efficiencies of the UV emission bands differ.
Source: Data from Christensen et al. (2023).

emission ratio similarly to a slightly higher LET. Consequently, the effect of overlapping tracks above a certain dose threshold cannot be distinguished from the effect of LET. For both Al_2O_3:C and Al_2O_3:C,Mg OSLDs, this effect occurs above a certain threshold, typically around 1 Gy to 2 Gy for mono-energetic proton fields (Flint et al., 2016). The approximate dose linearity region of the Al_2O_3:C and Al_2O_3:C,Mg OSLDs is outlined in Fig. 2a. For heavier ions with higher stopping power, the corresponding thresholds scale by the stopping power ratio. In carbon ion beam therapy, both $\overline{LET}$ determinations and dosimetry can be conducted at doses up to several grays without affecting the UV/blue emission ratio.

However, an LET determination outside the linearity region in Fig. 2a can be conducted in two ways: (i) either by experimentally calibrating the OSLDs at the dose of interest or, more generally, (ii) correcting the dose with a theoretically based model. In the case of the latter, the response of the OSLD emission bands to a certain dose and mixed particle field can be assessed numerically using compound Poisson modeling (Greilich et al., 2014), and correction factors concerning the dose linearity region determined. Nonetheless, the determination of $\overline{LET}$ outside the dose linearity region is associated with larger uncertainty, which can be avoided by reducing the radiation field dose when possible.

3.2. Signal fading and build-up

One of the challenges with $\overline{LET}$ determination using Al_2O_3:C is the build-up of the UV emission band (Granville, 2015; Christensen et al., 2022). Due to the low fading rate of the blue emission band, the ratio of the UV/blue emission of Al_2O_3:C OSLDs increases with time after irradiation, as depicted in Fig. 2b. If multiple OSLDs are read out over several days post-irradiation, this build-up could lead to variations of up to 20% between OSLDs irradiated under the same radiation quality conditions. To mitigate this, Al_2O_3:C OSLDs are typically read out in a window starting 14 days after irradiation, minimizing the variation among the OSLDs. The typical readout window for the Al_2O_3:C OSLDs is outlined in Fig. 2b.

In contrast, the build-up of the UV emission band for Al_2O_3:C,Mg differs significantly from that of Al_2O_3:C, as illustrated in Fig. 2b. For Al_2O_3:C,Mg, the UV/blue ratio remains relatively stable over time, allowing for OSLD readout shortly after irradiation and requiring smaller corrections for build-up compared to Al_2O_3:C. Nonetheless, although the variation of the UV/blue ratio over time is small for Al_2O_3:C,Mg, the low build-up or fading rate of the signal still needs to be corrected with respect to a certain time, which gives correction factors within 1%.

Although the dose response is similar for both Al_2O_3:C and Al_2O_3:C,Mg, the lower build-up rate of Al_2O_3:C,Mg enables a more accurate determination of radiation quality through the correction factors closer to unity. Furthermore, the stability of the UV/blue ratio over time allows for more flexibility of the readouts post irradiation.

3.3. Relative luminescence efficiency

For ion beam dosimetry with solid-state detectors, the reduction or increase of detector efficiency with varying ionization densities requires corrections. Fig. 3 illustrates the relative luminescence efficiencies for both the blue and UV emission intensities for Al_2O_3:C and Al_2O_3:C,Mg OSLDs.

The relative intensity of the blue emission band decreases with increasing ionization density as parameterized through $\overline{LET}_F$ in Fig. 3a for measurements in proton, helium, and carbon ions. While the blue OSL intensity of Al_2O_3:C and Al_2O_3:C,Mg is similar, the situation differs for the UV band, where particularly the UV emission from Al_2O_3:C would be difficult to use for dosimetry.

However, if the radiation quality can be determined, e.g. through $\overline{LET}_F$, then the characterization of the luminescence efficiency can be used as a look-up table as in Fig. 3 for the ionization quenching correction factor for dosimetry in ion beams.

4. Radiation quality metrics

An assessment of the radiation quality in ion beams is useful for both dosimetry or to estimates parameters relevant for radiobiological studies. Most studies in proton therapy characterize radiation quality through $\overline{LET}_D$ (Rørvik et al., 2018; Mohan, 2022). However, $\overline{LET}$ is not an ideal descriptor in mixed particle fields or even at spread-out Bragg peaks, where different ion types with the same LET exhibit distinct track structures and thus result in different ionization densities and finally different detector responses for the same $\overline{LET}$.

$\overline{LET}_D$, particularly, exhibits an elevated sensitivity to the presence of nuclear fragments compared to $\overline{LET}_F$ (Grzanka et al., 2018). This

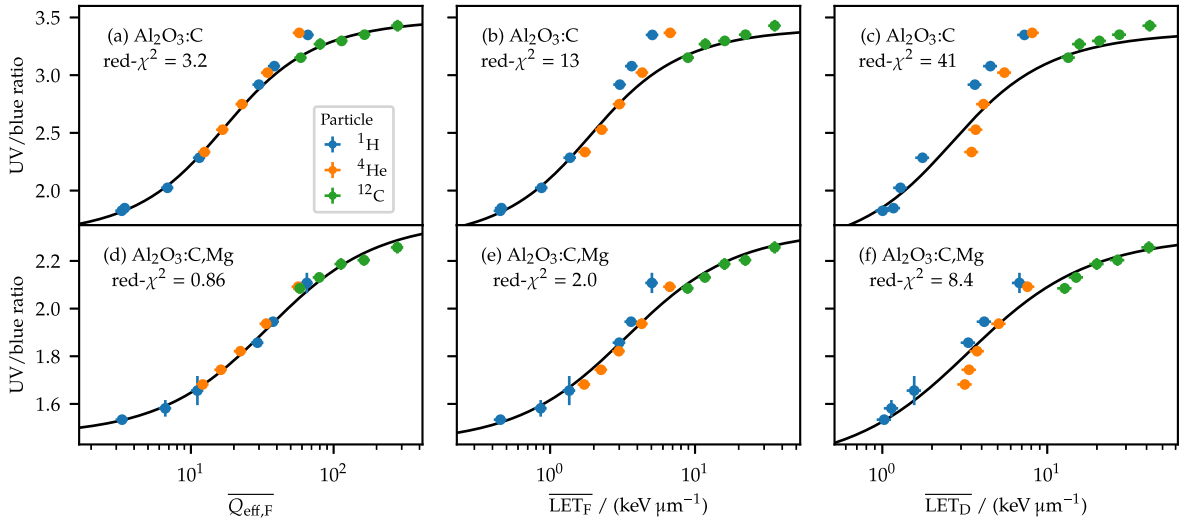

Fig. 4. Correlation between the UV/blue emission ratio and three radiation quality metrics for both Al_2O_3:C and Al_2O_3:C,Mg. The data is in each case modeled with a logistic function with its reduced χ^2-value given in the subplot. The best correlation is found for $Q_{eff,F}$ for Al_2O_3:C,Mg, i.e. it enables the most accurate quenching correction and consequently more accurate dosimetry.
Source: Data from Christensen et al. (2023).

characteristic renders it a challenging metric for assessing the radiation quality for passive luminescence detectors in mixed particle fields. In such radiation fields, heavy secondary particles contribute relatively less to the luminescence signal, due to ionization quenching, in contrast to low-LET particles, see Fig. 3. The challenge arises as the opposite effect is observed for $\overline{LET}_D$ in proton therapy, where the presence of heavy secondaries is far from negligible and may even double the magnitude of $\overline{LET}_D$ (Grzanka et al., 2018). This implies that $\overline{LET}_F$ is a better radiation quality metric than $\overline{LET}_D$ for passive luminescence detectors in mixed particle fields, as $\overline{LET}_F$ is less sensitive to the contributions from high-LET components, which aligns with the experimentally derived conclusions in Christensen et al. (2023).

Consequently, $\overline{LET}$ is not a good predictor of the integral response of passive detectors in mixed particle fields, and also exhibits problems in radiobiology (Grün et al., 2019; Kalholm et al., 2023).

To address this challenge, the radiation quality metric

$$Q_{\text{eff}} = \frac{z^{*2}}{\beta^2}, \quad \text{with} \quad z^*(\beta) = z\left(1 - \exp\left(-\frac{125\beta}{z^{2/3}}\right)\right), \tag{1}$$

where β represents the fraction of the relativistic speed of the ion with charge z, has been investigated as a potential improvement for dosimetry with OSLDs (Christensen et al., 2023). Q_{eff} is independent of material density and has been used for decades to describe ion track structures (Barkas, 1963).

Recently, Q_{eff} was shown to better predict the relative biological effectiveness of *in vitro* cells irradiated with protons compared to the $\overline{LET}$ (Kalholm et al., 2023). Motivated by this study, the responses of Al_2O_3:C and Al_2O_3:C,Mg OSLDs to light ions were examined to identify a more suitable radiation quality metric (Christensen et al., 2023).

Fig. 4 illustrates the relationship between the ratio of the UV and blue emission intensities, see e.g. Fig. 3, plotted against the radiation quality. The radiation quality has been parameterized as Q_{eff} averaged with respect to fluence ($Q_{\text{eff,F}}$) as well as the commonly used $\overline{LET}_F$ and $\overline{LET}_D$. The figure displays the response of Al_2O_3:C and Al_2O_3:C,Mg OSLDs irradiated with ^{1}H, ^{4}He, and ^{12}C ions as detailed in a previous publication (Christensen et al., 2023). Each data point in Fig. 4 represents the mean and standard deviation of the UV/blue ratio for a package containing 4–8 OSLDs.

Following an empirical approach, the data in each group was fitted with a tangential function. The quality of the fit is presented as the reduced χ^2 reported in the legend of each subplot. For the Al_2O_3:C OSLD data across the three radiation quality metrics, particularly evident in Fig. 4c for $\overline{LET}_D$, the OSLD response is separated into distinct groups for each ion type. This segmentation complicates the establishment of a unique calibration for the given radiation quality metric as it becomes challenging to relate the response to a singular value, which poses a challenge for measurements in mixed particle fields.

However, the situation markedly improves for the Al_2O_3:C,Mg OSLD data parameterized for $Q_{\text{eff,F}}$ in Fig. 4d. Here, the responses for the three ion types appear well-approximated by a single function, facilitating the determination of $Q_{\text{eff,F}}$ in mixed radiation fields relevant to carbon ion therapy. Consequently, carbon ion beam therapy dosimetry is more accurate when the ionization quenching corrections are derived from $Q_{\text{eff,F}}$ rather than from $\overline{LET}_F$ or $\overline{LET}_D$. Further discussion on these results can be found in a previous publication (Christensen et al., 2023).

5. OSLD applications in ion beam therapy

The utilization of Al_2O_3:C,Mg OSLDs in conjunction with an improved readout and analysis technique enables more accurate dosimetry compared to previous methodologies with Al_2O_3:C OSLDs, thus facilitating dosimetry of carbon ion beams. This improvement can be attributed to the following key factors:

(i) Implementation of the reference irradiation technique S/S_R, enhancing readout precision, as depicted in Fig. 1 and demonstrated in Christensen et al. (2022).

(ii) Negligible build-up rate of Al_2O_3:C,Mg relative to Al_2O_3:C, allowing for faster readout in combination with smaller correction factors as reported in Fig. 2.

(iii) Differential response of Al_2O_3:C,Mg to light ions compared to Al_2O_3:C, illustrated in Fig. 4d, and further discussed by Christensen et al. (2023).

(iv) Introduction of the radiation quality metric Q_{eff}, providing more accurate ionization quenching correction factors compared to averaged LET (Christensen et al., 2023).

The ability to determine $\overline{LET}_F$ and $\overline{LET}_D$ with OSLDs was recently compared to other passive luminescence detectors across the relevant proton therapy radiation qualities (Muñoz et al., 2024). For a review of the possibilities for radiation quality determinations with both passive and active detectors, the readers are referred to Christensen et al. (2024).

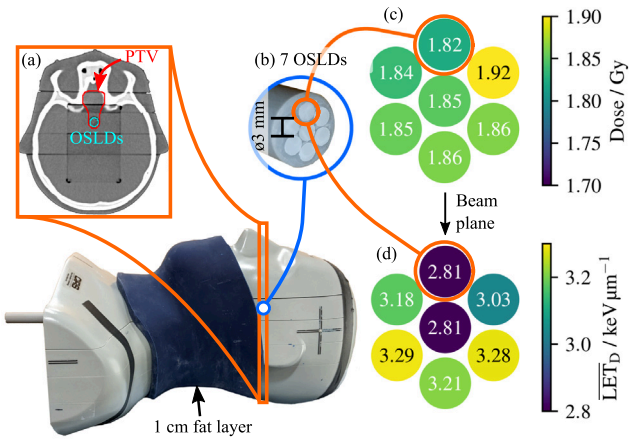

Fig. 5. Quality assurance of adaptive proton therapy using OSLDs. (a) Illustrates the planning target volume (PTV) outlined in red and the OSLD positions outlined in teal on a CT slide of the head-and-neck phantom. (b) Photo of seven 3 mm diameter OSLDs used to experimentally validate the planned dose and $\overline{LET}_D$. (c) and (d) show the determined dose and $\overline{LET}_D$, respectively, for the seven OSLDs for one treatment fraction delivery. The beam plane is outlined over (d). The prescribed dose to the target volume was 1.82 Gy, whereas the $\overline{LET}_D$ varied throughout the target volume.
Source: Figure replotted from Bobić et al. (2024).

5.1. OSLDs for proton therapy

The OSLDs were utilized to experimentally validate a workflow for adaptive proton therapy at PSI using an anthropomorphic head-and-neck phantom (Bobić et al., 2024). The phantom enabled a filling of the nasal cavities to simulate nasal congestion or adding a 1 cm fat layer around the neck to mimic a weight gain, see Fig. 5. The OSLDs were positioned inside the target volume within the phantom (Fig. 5a) to assess both dose and $\overline{LET}_D$ under different geometrical configurations to simulate different daily variations.

The objective of the study was to ensure that the online adaptive proton therapy workflow correctly adapts to the geometrical changes of the phantom, ensuring accurate delivery of the prescribed dose fraction of 1.82 Gy to the target volume.

Given the well-defined behavior of both Al_2O_3:C and Al_2O_3:C,Mg OSLDs in response to protons, as depicted in Fig. 4, both types of OSLDs could be employed. For each geometrical configuration of the phantom, seven 3 mm-diameter and <100 µm thin OSLDs were mounted on a rod and positioned at the target volume, as shown in Fig. 5b.

For each OSLD, both the dose, reduced by ionization quenching, and the radiation quality metrics $Q_{eff,F}$ and $\overline{LET}_D$ were determined. The $\overline{LET}_D$ values derived from the OSLDs, through a fit to the proton data in Fig. 4c, and were utilized to validate the reference $\overline{LET}_D$ obtained with a Monte Carlo particle transport code (Bobić et al., 2024). Following these findings, ionization quenching correction factors were determined from the $Q_{eff,F}$ values (Christensen et al., 2023).

The doses, after ionization quenching corrections, and $\overline{LET}_D$ values from one treatment fraction delivery are illustrated in Fig. 5c–d, respectively. The variations in $\overline{LET}_D$ reflect the different proton energy distributions throughout the spread-out Bragg peak. In Fig. 5d, the three fields were directed from above, in a plane indicated by an arrow, meaning that the highest LET values should be measured at the lower three OSLDs, which is consistent with the measured data. The experimentally determined $\overline{LET}_D$ values were all found to agree with the simulated $\overline{LET}_D$ in the target volume: on average, the OSLD-determined doses and $\overline{LET}_D$ values were within 1.4% and 3.2% of the simulated values, respectively, for the 42 OSLDs. Detailed information on the radiation fields and additional results can be found in Bobić et al. (2024).

These findings demonstrate that Al_2O_3:C- and Al_2O_3:C,Mg-based OSLDs, are applicable for both dosimetry and radiation quality determination in proton therapy. Their passive nature, high precision, and accuracy make them suitable for measurements within anthropomorphic phantoms with minimal disturbance to the radiation field due to a thickness below 100 µm.

5.2. OSLDs for carbon ion therapy

Dosimetry in carbon ion beams presents challenges due to elevated ionization densities, leading to significant ionization quenching in solid-state detectors, and consequent underestimation of the dose (Vedelago et al., 2022; Yukihara et al., 2022a). However, utilizing OSLDs to determine radiation quality through the UV/blue ratio enables estimation of the required quenching correction factors for dosimetry. With the introduction of Al_2O_3:C,Mg OSLDs and the radiation quality metric Q_{eff}, it became feasible to correlate the UV/blue ratio response to radiation quality across ions relevant to carbon ion therapy (Christensen et al., 2023), as depicted in Fig. 4a,d.

The feasibility of OSLD dosimetry for carbon ion therapy was assessed using a recently developed phantom, the abdominal Pancreas Phantom for Ion beam Therapy (PPIeT) (Stengl et al., 2023, 2024). The aim was to evaluate novel treatment modalities for pancreatic cancer using a phantom that can mimic breathing-induced organ motion. Key components of the anthropomorphic phantom PPIeT, outlined in Fig. 6, comprise a pancreas with a virtual tumor, and its organs at risk (OARs), including the duodenum, the two kidneys, the spine, and the spinal cord. These organs are suspended in a superabsorber-water mixture that makes it possible to induce motion through a motor system connected to the phantom, reproducing arbitrary breathing patterns (Stengl et al., 2023). Each organ contains 3D-printed inserts to accommodate between 3 and 12 OSLDs, as illustrated in Fig. 6.

The initial tests were done with no motion induced in the organs while delivering one treatment fraction for the virtual tumor at the pancreas. In each of these measurements, a total of 53 Al_2O_3:C,Mg OSLDs were placed in the organ inserts to measure the dose at the target and organs at risk.

To validate the OSLD workflow for carbon ion beam dosimetry, the dose to the pancreas was measured with an ionization chamber. The pancreas OSLD insert in Fig. 6 was swapped with an insert for the ionization chamber, which enabled measurements of the dose in the same positions as the OSLDs in the target volume. After ionization quenching corrections through $Q_{eff,F}$, the preliminary OSLD doses were in agreement with the ionization chamber measured dose within 2%, which also validates the assessment of the radiation quality through OSLDs, later used in turn to determine the dose correction factors.

6. Outlook and ongoing projects

The recent advancements in dosimetry using OSLDs have enabled several ongoing innovative projects. The dose-rate independence of Al_2O_3:C OSLDs (Christensen et al., 2021; Motta et al., 2024) has facilitated the development of a postal audit set for dosimetry of FLASH proton beams for an ongoing inter-comparison. The passive nature of OSLDs allowed for the development of the first postal LET audit kit, utilizing both Al_2O_3:C and Al_2O_3:C,Mg OSLDs.

One extra advantage of the passive nature of OSLDs is that they can be embedded within anthropomorphic phantom as illustrated in Figs. 5 and 6. Particular the possibility for dosimetry with OSLDs inserted in the abdominal phantom PPIeT, where different breathing motion patterns can be applied during carbon ion therapy to investigate the effect of beam gating on dose distributions in pancreatic cancer scenarios. Dosimetry inside the phantom is not feasible with detectors without an inherent way of correction the response for the elevated ionization densities relevant to carbon ions.

The dose dependency of the UV/blue ratio, which generally occurs above 2 Gy for protons (Flint et al., 2016) and disturbs the $\overline{LET}$ determination, can theoretically be corrected with different approaches, e.g. compound Poisson processes (Greilich et al., 2014)

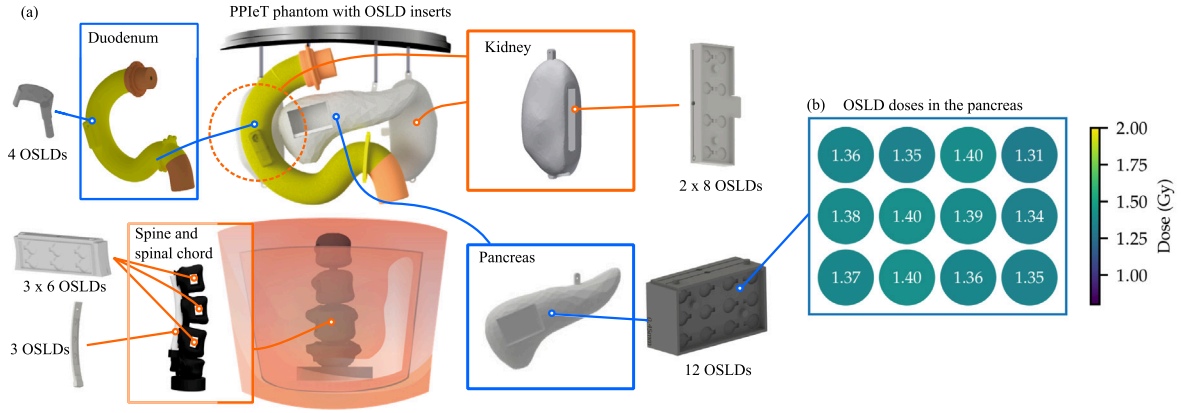

Fig. 6. (a) Overview of the abdominal pancreas phantom PPIeT for carbon ion therapy. A total of 53 OSLDs for dosimetry can be embedded inside the pancreas, the duodenum, two kidneys, the spine and the spinal cord. Figure replotted from Stengl et al. (2023). (b) Example of dose measurements with the 12 OSLDs placed in the pancreas, where corrections for ionization quenching have been employed. Numbers in the circle represent the dose to that OSLD in units of Gray. The planned dose was 1.36 Gy.

OSL dosimetry. Other OSL systems have been demonstrated for dosimetry based on KCl:Eu^{2+} (Xiao et al., 2014) or enabling a low signal fading with a precision better than 2% using BeO (Jahn et al., 2013). Ahmed et al. (2014) demonstrated that Al_2O_3:C OSL films enable two-dimensional dose measurements with high spatial resolution. This technique is currently being enhanced to establish two-dimensional, simultaneous dose and LET determination, potentially improving future measurements in ion beam therapy, particularly in the context of treatment planning system validation.

Besides Al_2O_3:C and Al_2O_3:C,Mg OSL foils, two-dimensional OSL dosimetry systems have been demonstrated using various materials including $LiMgPO_4$ (Sądel et al., 2023), $NaMgF_3$:Eu (Schuyt and Williams, 2019), and MgB_4O_7:Ce,Li (Shrestha et al., 2020). Notably, Wouter et al. (2017) showed that an OSL film based on BaFBr provided a sub-mm resolution and higher accuracy than radiochromic film while also being reusable. Recently, a three-dimensional system for OSL dosimetry relying on YSO:Ce was showcased (Jensen et al., 2023).

Quality assurance. The current capability to measure both dose and $\overline{\text{LET}}$ with OSLDs allows for yearly quality assurance (QA) or commissioning of treatment planning systems. The passive nature of OSLDs facilitates a postal QA or audit of both dose and $\overline{\text{LET}}$, independent of dose rate, and extends up to doses pertinent to delivering a 2 Gy fraction. While OSLDs presently enable QA of complex $\overline{\text{LET}}$ distributions within anthropomorphic phantoms through multiple point-like measurements, the advancement towards a two-dimensional dose and $\overline{\text{LET}}$ OSL system will greatly enhance its relevance in ion beam therapy QA efforts.

Conclusion

The recent advancement of optically stimulated luminescence detectors (OSLDs) based on Al_2O_3:C,Mg has enhanced their applicability in ion beam dosimetry and $\overline{\text{LET}}$ determination. Whereas the use of Al_2O_3:C OSLDs faced challenges, in particular, due to the divergent responses to different ion types, the application of Al_2O_3:C,Mg OSLDs overcomes most of these issues.

Both types of OSLDs offer precise measurements, with the well-known S/S_R technique improving accuracy. However, the distinct advantage of Al_2O_3:C,Mg OSLDs lies in the negligible build-up rate compared to Al_2O_3:C OSLDs, reducing both correction requirements and waiting times for readout.

Moreover, the ability to model the response of Al_2O_3:C,Mg OSLDs to various ion types with a single function enables an estimation of the radiation quality. An accurate determination of radiation quality is crucial for determining ionization quenching correction factors necessary for dosimetry in carbon ion beams with OSLDs.

The advancements of the last years have enabled the integration of OSLDs into anthropomorphic phantoms to support both proton and carbon ion beam therapy with independent measurements of the dose and simultaneous determination of the radiation quality.

CRediT authorship contribution statement

Jeppe Brage Christensen: Writing – review & editing, Writing – original draft, Visualization, Validation, Supervision, Software, Resources, Project administration, Methodology, Investigation, Formal analysis, Data curation, Conceptualization. **Lily Bossin:** Writing – review & editing, Writing – original draft, Investigation, Data curation. **Iván Domingo Muñoz:** Writing – review & editing, Writing – original draft, Investigation, Data curation. **Christina Stengl:** Writing – review & editing, Writing – original draft, Visualization, Investigation, Data curation. **José Vedelago:** Writing – review & editing, Writing – original draft, Investigation, Data curation. **Eduardo Gardenali Yukihara:** Writing – review & editing, Writing – original draft, Validation, Supervision, Resources, Project administration, Methodology, Investigation, Funding acquisition, Formal analysis, Data curation, Conceptualization.

Declaration of competing interest

E. G. Yukihara is co-Editor-in-Chief and José Vedelago is a member of the Early Career Editorial Board for Radiation Measurements; neither was involved in the editorial review or the decision to publish this article.

Data availability

Data will be made available on request.

Acknowledgments

The OSLDs were read out with a Risø TL/OSL-DA-20 reader (DTU Nutech, Denmark) acquired with partial support from the Swiss National Science Foundation (R'Equip project 206021_177028). The authors thank Alexander Neuholz and Stephan Brons from HIT for their support with the irradiations of PPIeT.

References

Ahmed, M.F., Eller, S.A., Schnell, E., Ahmad, S., Akselrod, M.S., Hanson, O.D., Yukihara, E.G., 2014. Development of a 2D dosimetry system based on the optically stimulated luminescence of Al_2O_3. Radiat. Meas. 71, 187–192.

Akselrod, M.S., Akselrod, A.E., 2006. New Al_2O_3:C,Mg crystals for radiophotoluminescent dosimetry and optical imaging. Radiat. Prot. Dosim. 119, 218–221.

Barkas, H.W., 1963. Nuclear Research Emulsions. Vol. 1 ed., Academic Press, New York and London.

Bobić, M., Christensen, J.B., Lee, H., Choulilitsa, E., Czerska, K., Togno, M., Safai, S., Yukihara, E.G., Winey, B.A., Lomax, A.J., et al., 2024. Optically stimulated luminescence dosimeters for simultaneous measurement of point dose and dose-weighted LET in an adaptive proton therapy workflow. Front. Oncol. 13, 1333039.

Christensen, J.B., Muñoz, I.D., Bassler, N., Stengl, C., Bossin, L., Togno, M., Safai, S., Jäkel, O., Yukihara, E.G., 2023. Optically stimulated luminescence detectors for dosimetry and LET measurements in light-ion beams. Phys. Med. Biol. 68, 155001.

Christensen, J.B., Muñoz, I.D., Bilski, P., Conte, V., Olko, P., Bossin, L., Vestergaard, A., Agosteo, S., Rosenfeld, A., Tran, L., Knezevic, Z., Majer, M., Ambrozova, I., Parisi, A., Gehrke, T., Martisikova, M., Bassler, N., 2024. Status of LET assessment with active and passive detectors in ion beams. Radiat. Meas. 177, 107252.

Christensen, J.B., Togno, M., Bossin, L., Pakari, O.V., Safai, S., Yukihara, E.G., 2022. Improved simultaneous LET and dose measurements in proton therapy. Sci. Rep. 12, 1–10.

Christensen, J.B., Togno, M., Nesteruk, K.P., Psoroulas, S., Meer, D., Weber, D.C., Lomax, T., Yukihara, E.G., Safai, S., 2021. Al_2O_3:C optically stimulated luminescence dosimeters (OSLDs) for ultra-high dose rate proton dosimetry. Phys. Med. Biol. 66.

Edmund, J., Andersen, C., Marckmann, C., Aznar, M., Akselrod, M., Bøtter-Jensen, L., 2006. CW-OSL measurement protocols using optical fibre Al_2O_3:C dosemeters. Radiat. Prot. Dosim. 119, 368–374.

Flint, D.B., Granville, D.A., Sahoo, N., McEwen, M., Sawakuchi, G.O., 2016. Ionization density dependence of the curve shape and ratio of blue to UV emissions of Al_2O_3:C optically stimulated luminescence detectors exposed to 6-MV photon and therapeutic proton beams. Radiat. Meas. 89, 35–43.

Granville, D.A., 2015. Development of a Technique To Simultaneously Verify Linear Energy Transfer and Absorbed Dose in Therapeutic Proton Beams (Ph.D. thesis). Carleton University.

Granville, D.A., Sahoo, N., Sawakuchi, G.O., 2014. Linear energy transfer dependence of Al_2O_3:C optically stimulated luminescence detectors exposed to therapeutic proton beams. Radiat. Meas. 71, 69–73.

Granville, D.A., Sahoo, N., Sawakuchi, G.O., 2016. Simultaneous measurements of absorbed dose and linear energy transfer in therapeutic proton beams. Phys. Med. Biol. 61, 1765–1779.

Greilich, S., Hahn, U., Kiderlen, M., Andersen, C.E., Bassler, N., 2014. Efficient calculation of local dose distributions for response modeling in proton and heavier ion beams. Eur. Phys. J. D 68, 0–4.

Grün, R., Friedrich, T., Traneus, E., Scholz, M., 2019. Is the dose-averaged LET a reliable predictor for the relative biological effectiveness? Med. Phys. 46, 1064–1074.

Grzanka, L., Ardenfors, O., Bassler, N., 2018. Monte Carlo simulations of spatial LET distributions in clinical proton beams. Radiat. Prot. Dosim. 180, 296–299.

Jahn, A., Sommer, M., Ullrich, W., Wickert, M., Henniger, J., 2013. The BeOmax system–dosimetry using OSL of BeO for several applications. Rad. Meas. 56, 324–327.

Jensen, M.L., Julsgaard, B., Turtos, R.M., Skyt, P.S., Jensen, M.B., Muren, L.P., Balling, P., 2023. High-resolution three-dimensional dosimetry in clinically relevant volumes utilizing optically stimulated luminescence. Med. Phys. 51 (3), 2200–2209.

Kalholm, F., Grzanka, L., Toma-Dasu, I., Bassler, N., 2023. Modeling RBE with other quantities than LET significantly improves prediction of in vitro cell survival for proton therapy. Med. Phys. 50 (1), 651–659.

Mohan, R., 2022. A review of proton therapy–current status and future directions. Precis. Radiat. Oncol. 6, 164–176.

Motta, S., Christensen, J., Yukihara, E., 2023. Testing the S/S_R procedure using TLDs and OSLDs and a lexsyg smart automated reader for precise dosimetry. Radiat. Meas. 168, 107013.

Motta, S., Dal Bello, R., Christensen, J.B., Bossin, L., Yukihara, E.G., 2024. Dosimetry of ultra-high dose rate electron beams using thermoluminescence and optically stimulated luminescence detectors. Phys. Med. Biol. 69, 035022.

Muñoz, I.D., van Hoey, O., Parisi, A., Bassler, N., Grzanka, N., de Saint-Hubert, M., Vaniqui, A., Olko, P., Sadel, M., Stolarczyk, L., Vestergaard, A., Jäkel, O., Yukihara, E.G., Christensen, J.B., 2024. Assessment of fluence- and dose-averaged linear energy transfer with passive luminescence detectors in clinical proton beams. Phys. Med. Biol. 69 (13), 135004.

Rørvik, E., Fjæra, L.F., Dahle, T.J., Dale, J.E., Engeseth, G.M., Stokkevåg, C.H., Thörnqvist, S., Ytre-Hauge, K.S., 2018. Exploration and application of phenomenological RBE models for proton therapy. Phys. Med. Biol. 63, 185013.

Sądel, M., Grzanka, L., Swakoń, J., Baran, J., Gajewski, J., Bilski, P., 2023. Optically stimulated luminescent response of the $LiMgPO_4$ silicone foils to protons and its dependence on proton energy. Materials 16, 1978.

Sawakuchi, G., Sahoo, N., Gasparian, P., Rodriguez, M., Archambault, L., Titt, U., Yukihara, E., 2010. Determination of average LET of therapeutic proton beams using Al_2O_3:C optically stimulated luminescence (OSL) detectors. Med. Phys. 37, 3453.

Sawakuchi, G.O., Yukihara, E., McKeever, S., Benton, E., Gaza, R., Uchihori, Y., Yasuda, N., Kitamura, H., 2008. Relative optically stimulated luminescence and thermoluminescence efficiencies of Al_2O_3:C dosimeters to heavy charged particles with energies relevant to space and radiotherapy dosimetry. J. Appl. Phys. 104, 124903.

Schuyt, J., Williams, G., 2019. Development of a 2D dosimeter using the optically stimulated luminescence of $NaMgF_3$:Eu with CCD camera readout. Radiat. Meas. 121, 99–102.

Shrestha, N., Vandenbroucke, D., Leblans, P., Yukihara, E., 2020. Feasibility studies on the use of MgB_4O_7:Ce, Li-based films in 2D optically stimulated luminescence dosimetry. Phys. Open 5, 100037.

Stengl, C., Muñoz, I.D., Arbes, E., Rauth, E., Christensen, J.B., Vedelago, J., Runz, A., Jäkel, O., Seco, J., 2024. Dosimetric study for breathing-induced motion effects in an abdominal pancreas phantom for carbon ion mini-beam radiotherapy. Med. Phys. 51, 5618–5631.

Stengl, C., Panow, K., Arbes, E., Muñoz, J.B., Neelsen, C., Dinkel, F., Weidner, A., Runz, A., Johnen, W., et al., 2023. A phantom to simulate organ motion and its effect on dose distribution in carbon ion therapy for pancreatic cancer. Phys. Med. Biol. 68, 245013.

Vedelago, J., Karger, C., Jäkel, O., 2022. A review on reference dosimetry in radiation therapy with proton and light ion beams: status and impact of new developments. Radiat. Meas. 157, 106844.

Wouter, C., Dirk, V., Paul, L., Tom, D., 2017. A reusable OSL-film for 2D radiotherapy dosimetry. Phys. Med. Biol. 62, 8441.

Xiao, Z., Hansel, R., Zhang, L., Li, H.H., 2014. Temperature dependence of the photostimulated luminescence in $KCl:Eu^{2+}$. Nucl. Instrum. Methods Phys. Res. B 326, 182–184.

Yasuda, H., Kobayashi, I., 2001. Optically stimulated luminescence from Al_2O_3:C irradiated with relativistic heavy ions. Radiat. Prot. Dosim. 95, 339–343.

Yukihara, E.G., Christensen, J.B., Togno, M., 2022a. Demonstration of an optically stimulated luminescence (OSL) material with reduced quenching for proton therapy dosimetry: MgB_4O_7:Ce, Li. Radiat. Meas 152, 106721.

Yukihara, E.G., Doull, B.A., Ahmed, M., Brons, S., Tessonnier, T., Jäkel, O., Greilich, S., 2015. Time-resolved optically stimulated luminescence of Al_2O_3:C for ion beam therapy dosimetry. Phys. Med. Biol. 60, 6613–6638.

Yukihara, E.G., McKeever, S.W.S., 2006. Spectroscopy and optically stimulated luminescence of Al_2O_3:C using time-resolved measurements. J. Appl. Phys. 100, 083512.

Yukihara, E.G., McKeever, S.W.S., Andersen, C.E., Bos, A.J.J., Bailiff, I.K., Yoshimura, E.M., Sawakuchi, G.O., Bossin, L., Christensen, J.B., 2022b. Luminescence dosimetry. Nat. Rev. Methods Primers 2.

Yukihara, E.G., Sawakuchi, G.O., Guduru, S., McKeever, S.W.S., Gaza, R., Benton, E.R., Yasuda, N., Uchihori, Y., Kitamura, H., 2006. Application of the optically stimulated luminescence (OSL) technique in space dosimetry. Radiat. Meas. 41, 1126–1135.

Yukihara, E.G., Yoshimura, E.M., Lindstrom, T.D., Ahmad, S., Taylor, K.K., Mardirossian, G., 2005. High-precision dosimetry for radiotherapy using the optically stimulated luminescence technique and thin Al_2O_3:C dosimeters. Phys. Med. Biol. 50, 5619–5628.